Breakup dynamic polarization potential for ^{6}He + ^{208}Pb: Energy dependence and generic properties

N. Keeley

CEA/DSM/DAPNIA/SPhN Saclay, 91191 Gif-sur-Yvette, France

R. S. Mackintosh*

Department of Physics and Astronomy,

The Open University, Milton Keynes, MK7 6AA, UK

(Dated: January 13, 2005)

Abstract

We extend to a series of higher energies an earlier study, R.S. Mackintosh and N. Keeley, Phys. Rev. **C 70**, 024604 (2004), of the local dynamic polarization potential for the ^{6}He + ^{208}Pb interaction. The dynamic polarization potential generated by the coupling to breakup channels is determined using the CDCC-plus-inversion method and does not involve semi-classical approximations. The long-ranged potential generated by the dipole breakup persists, with very little change in radial form and relative strength of real and imaginary terms, to energies far above the near Coulomb barrier energy of Ref. [1]. The dynamic polarization potentials presented here extend from 10 fm, well inside the SAR, out to 60 fm, i.e. including the transition region from where nuclear excitation dominates to the asymptotic region dominated by electric dipole excitation. Real and imaginary components of the dynamic polarization potential each contribute to the scattering,

PACS numbers: 24.10.-i, 25.10.+s, 25.60.-t, 24.50.+g

Keywords: ^{6}He, potential, dynamic polarization potential, breakup

* Electronic address: r.mackintosh@open.ac.uk

I. INTRODUCTION

In Ref. [1] we presented the dynamic polarization contribution to the interaction at 27 MeV between ^{6}He and ^{208}Pb that results from the breakup of the ^{6}He nucleus. In particular, EM dipole breakup contributed to the dynamic polarization potential, DPP, an exceptionally long tail with distinct radial forms for the real and imaginary parts. The real tail extended to at least 60 fm and the imaginary tail extended to 40 fm. In this brief report, we present extensions of these calculations to higher energies for at least two reasons: (1) semi-classical theories [2, 3, 4, 5] of dipole contributions to the DPP predict particular different energy dependences for the real and imaginary components; clearly, it is interesting to see if these are borne out by calculations not involving semi-classical assumptions, (2) the inversion method used to extract the DPP is expected to give smoother and better defined radial shapes at higher energies, making possible a more meaningful comparison with the radial form predicted by other methods. In addition, we have taken the opportunity to present the result of notch tests that specify the radial range over which our DPPs are well established. The inner sensitivity radius is well within both the strong absorption radius, SAR, and the radius within which nuclear coupling rather than Coulomb coupling determines the radial form of the DPP. Calculations at higher energies permit us to determine more accurately the nuclear DPP and determine its energy dependence. This will make it possible to compare DPPs for ^{6}He and ^{6}Li. In this paper, as in Ref. [1], we employ the IP $S_l \rightarrow V$ inversion procedure [6] to establish the DPP.

II. THE DPP FROM 27 MEV TO 66 MEV

We refer to Ref. [1] for a specification of the DPP at 27 MeV (but see Figures 1 – 3), but we comment here on the sensitive radial range over which the potential can be said to be determined: it is certainly not down to 0 fm. Notch tests at both 27 MeV and 40 MeV revealed that the differential cross-section was sensitive to the potentials from 10 fm outwards at both energies. The real and imaginary potentials seem to be well-determined for $r \geq 11$ fm. This should be compared to the SAR (based on $|S_L|^2 = 0.5$) which is ~ 13.1 fm at 27 MeV and ~ 12.4 fm at 40 MeV.

The initial 40 MeV calculations were based on bare interactions that vary with energy

in a realistic way. We examined how the energy dependence of the various model potentials propagates into the energy dependence of the DPP by repeating the 40 MeV calculations with all potentials identical to those used in the 27 MeV calculations. The real DPP using the 27 MeV bare potential was graphically almost indistinguishable, from 11.5 fm to 50 fm, from that based on the 40 MeV bare potential. The imaginary DPP had some differences in detail between 11.5 and 18 fm, but was identical from 18 fm to 50 fm. We conclude that, while there remains scope for exploring the dependence of the DPP on the details of the model potentials in the region where the nuclear potentials are significant, the general properties of the DPP in the overlap region and the precise properties of the tail are not affected by the energy dependence of the model potentials. The calculations with alternative (energy fixed and energy dependent) bare potentials, being independent calculations of the DPP, confirm that the long range DPP, where the DPP is determined by the E1 strength, is uniquely determined by inversion.

We evaluated the DPP for two further incident energy steps of 13 MeV with results shown in Figure 1 (for the lowest radial range for which it is reasonably well determined), in Figure 2 and in Figure 3 (for the extreme surface region). The wiggles in the 27 MeV imaginary part beyond 30 fm, where it is extremely small, are an artifact of the inversion; the curve shown is in fact an improved inversion with less oscillation than that in Ref. [1] which was shown only out to 40 fm. Figure 1 reveals that the DPP is both repulsive and emissive at all four energies between 10 and 13 fm. In this region, the 27 MeV DPPs (near the Coulomb barrier) did appear different in form to the three higher energy DPPs.

The energy dependence that emerges for the region beyond 15 fm can be summarized:

1. The real part of the DPP is not strongly energy dependent. In detail, it decreases with increasing energy between 20 and 30 fm but appears to increase with energy beyond 35 fm; there is, therefore, a tendency for it to fall most quickly with r at the lowest energy.

2. The imaginary DPP increases appreciably with energy for all $r > 15$ fm.

We note that, at energies far above the Coulomb barrier, the characteristic radial forms, different for the real and imaginary terms, remain qualitatively the same as they are at 27 MeV. Beyond 40 fm, the imaginary term is extremely small, but the real component falls off more slowly.

There are various ways our results could be compared with semiclassical results beyond comparing the above qualitative points. We offer to make our potentials available in tabu-

lated form.

III. CONTRIBUTIONS OF REAL AND IMAGINARY DPP TO SCATTERING

The individual contributions of the real and imaginary parts of the DPP to elastic scattering can be seen in Figure 4 which presents the elastic scattering differential cross-section from 10 to 30 degrees for four cases: the bare potential, the bare potential plus the real and imaginary parts of the DPP separately and the complete potential. The cross-sections follow the same pattern seen at the larger angles in Figure 4 out to at least 60 degrees, but the restricted angular scale of this figure reveals the behavior near the rainbow. In particular, the real and imaginary DPPs each attenuate the cross-section in the rainbow region to a comparable degree. However, beyond the rainbow, the real DPP increases the cross-section whereas the imaginary DPP lowers it. Beyond 24 degrees the *real* DPP 'wins' and the differential cross-section exhibits a much slower fall-off than that associated with the bare potential.

Close examination of the differential cross-section around 10 degrees reveals that here the effect of the real DPP is markedly greater than the effect of the imaginary term in accord with the longer range of the real DPP.

IV. GENERAL COMMENTS

Very little is known about the global and generic properties of the nucleus-nucleus dynamic polarization potential although such understanding is an essential ingredient in the more general understanding of nucleus-nucleus interactions. By its nature, the DPP represents contributions that cannot be accounted for in any folding model based on an underlying local density model. One not uncommon feature that appears in the present case is the existence of radial regions where the imaginary DPP is emissive.

In ref. [7], the appropriateness of the 'coupled channel plus inversion' method for studying the DPP was discussed and in Ref. [1] we applied this procedure to determine the DPP due to breakup for ^{6}He on ^{208}Pb at 27 MeV. A remarkable long range tail was found. We emphasize that this long ranged DPP is effectively uniquely determined as far as the inversion is concerned, any uncertainties lying with the model for ^{6}He. The general method

applied here can be applied to more complete models as they appear. For example, four-body CDCC calculations for ^{6}He + ^{12}C scattering have recently been published [8]. The formalism [8] does not currently include Coulomb excitation, but it will be interesting to see whether a more accurate model of the ^{6}He breakup process produces a qualitatively similar DPP. The CC plus inversion method using IP [6] inversion simultaneously yields the DPP both in the radial region accessible to semi-classical methods and in the inner region, in particular showing the very sharp crossover from the long range attraction to short range repulsion. A repulsive DPP frequently dominates in cases where breakup dominates but dipole excitation weak.

In this paper, we have presented the long range, dipole-generated DPP both near and above the Coulomb barrier, so that its radial and energy dependence can be compared with the predictions of semi-classical theories [2, 3, 4, 5]. In principle, where we can be sure that we are comparing models involving the same dipole excitation, this would provide an evaluation of the semi-classical approximations.

---

[1] R.S. Mackintosh and N. Keeley, Phys. Rev. **C 70**, 024604 (2004).

[2] O.R. Kakuee, J. Rahighi, A.M. Sánchez-Benítez, M.V. Andrés, S. Cherubini, T. Davinson, W. Galster, J. Gómez-Camacho, A.M. Laird, M. Lamehi-Rachti, I. Martel, A.C. Shotter, W.B. Smith, J. Vervier and P.J. Woods, Nucl. Phys. **A 728**, 339 (2003).

[3] M.V. Andrés, J. Gómez-Camacho and M.A. Nagarajan, Nucl. Phys. **A 579**, 273 (1994).

[4] L.F. Canto, R. Donangelo, P. Lotti and M.S. Hussein, Nucl. Phys. **A 589**, 117 (1995).

[5] W.G. Love, T. Terasawa and Satchler, Nucl. Phys. **A 291**, 183 (1977).

[6] V.I. Kukulin and R.S. Mackintosh, J. Phys. G: Nucl. Part. Phys. **30**, R1 (2004).

[7] R.S. Mackintosh and K. Rusek, Phys. Rev. **C 67**, 034607 (2003).

[8] T. Matsumoto, E. Hiyama, K. Ogata, Y. Iseri, M. Kamimura, S. Chiba and Y. Yahiro, Phys. Rev. **C 70**, 061601(R) (2004).

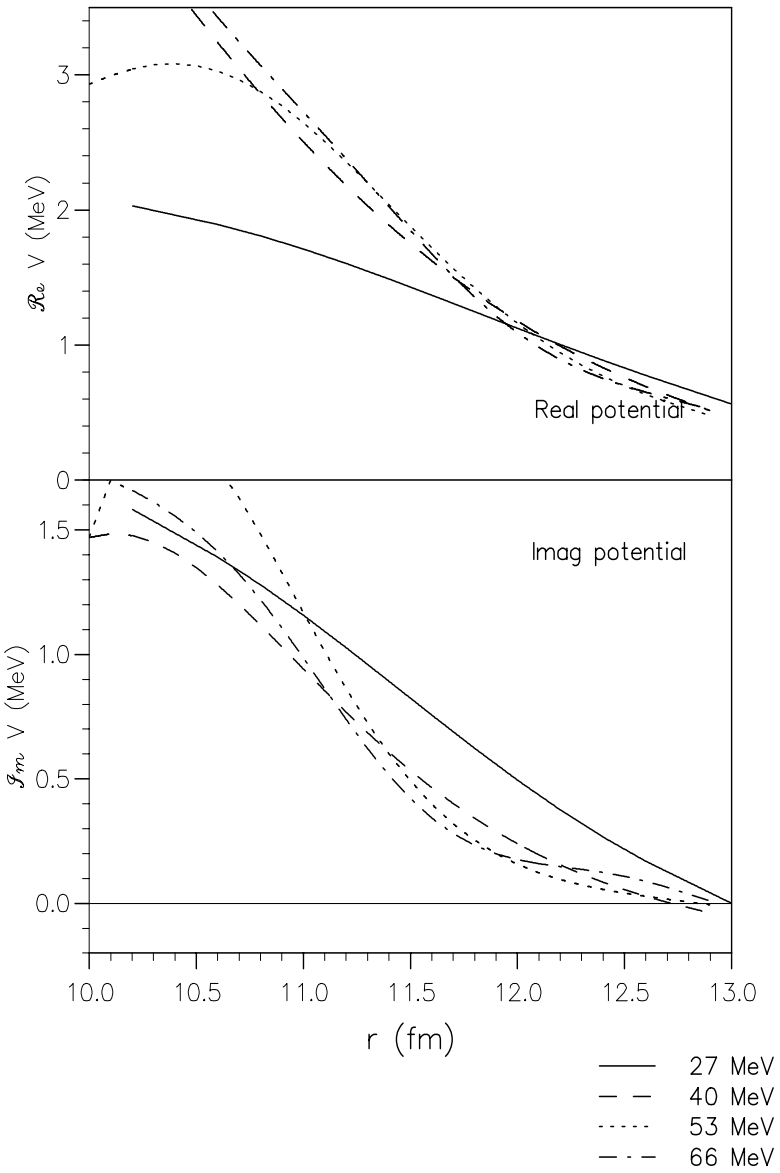

FIG. 1: The DPP at four energies, surface region.

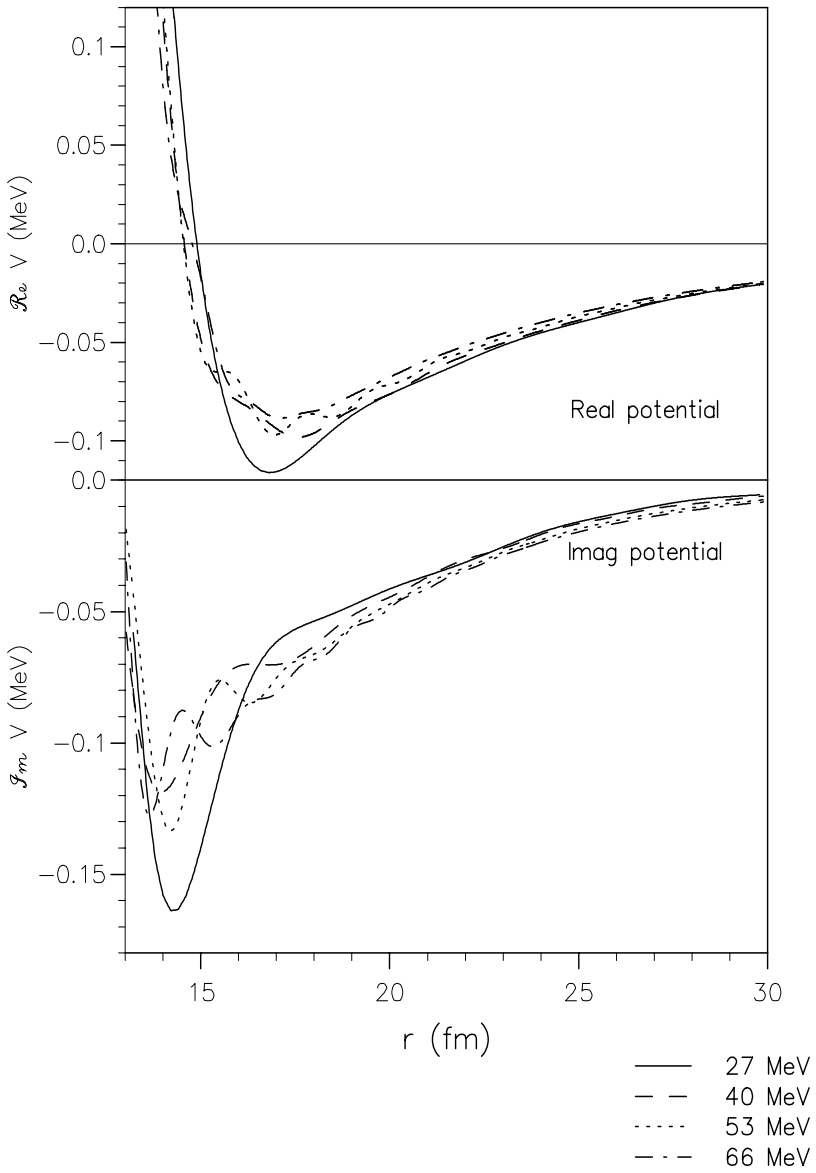

FIG. 2: The DPP at four energies, outer region.

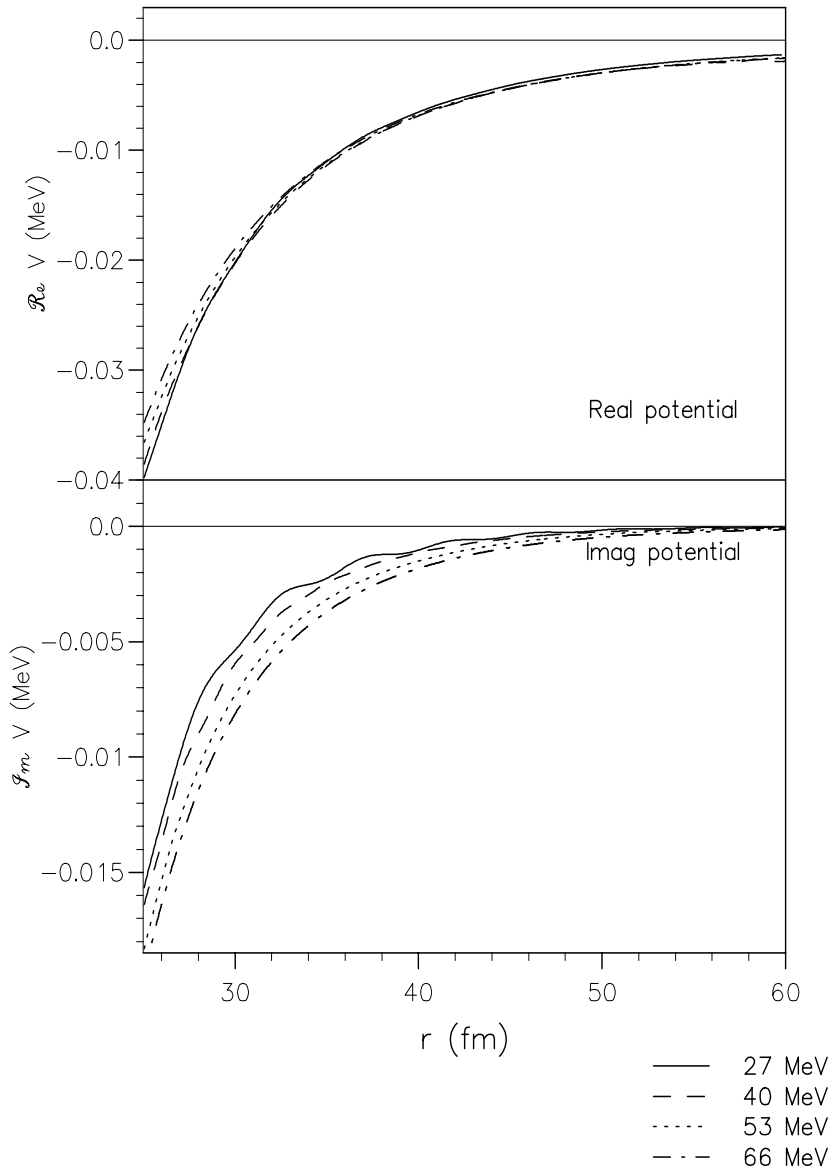

FIG. 3: The DPP at four energies, far region.

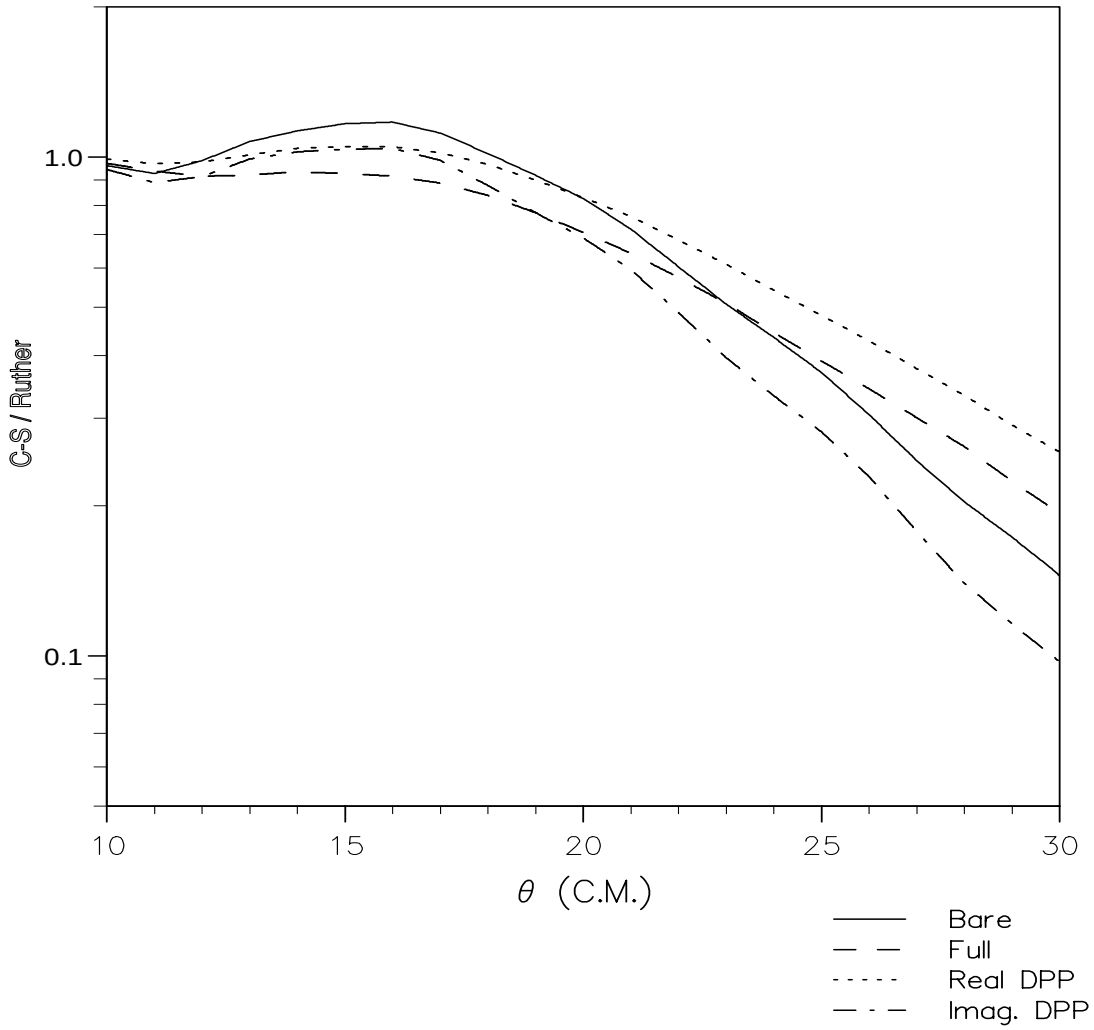

FIG. 4: For 53 MeV ^{6}He scattering from ^{208}Pb, the elastic scattering angular distributions showing the contributions of the real and imaginary parts of the DPP.